Journal of Biomolecular NMR (2006) 35: 137–147
DOI 10.1007/s10858-006-9008-y

Article

Dynamics of transportan in bicelles is surface charge dependent

Elsa Bárány-Wallje, August Andersson, Astrid Gräslund & Lena Mäler*
Department of Biochemistry and Biophysics, The Arrhenius Laboratories, Stockholm University, S-106 91 Stockholm, Sweden

Received 7 December 2005; Accepted 23 March 2006

Key words: bicelle, cell-penetrating peptide, dynamics, NMR, transportan

Abstract

In this study we investigated the dynamic behavior of the chimeric cell-penetrating peptide transportan in membrane-like environments using NMR. Backbone amide ^{15}N spin relaxation was used to investigate the dynamics in two bicelles: neutral DMPC bicelles and partly negatively charged DMPG-containing bicelles. The structure of the peptide as judged from CD and chemical shifts is similar in the two cases. Both the overall motion as well as the local dynamics is, however, different in the two types of bicelles. The overall dynamics of the peptide is significantly slower in the partly negatively charged bicelle environment, as evidenced by longer global correlation times for all measured sites. The local motion, as judged from generalized order parameters, is for all sites in the peptide more restricted when bound to negatively charged bicelles than when bound to neutral bicelles (increase in S^2 is on average 0.11 ± 0.07). The slower dynamics of transportan in charged membrane model systems cause significant line broadening in the proton NMR spectrum, which in certain cases limits the observation of ^{1}H signals for transportan when bound to the membrane. The effect of transportan on DMPC and DHPC motion in zwitterionic bicelles was also investigated, and the motion of both components in the bicelle was found to be affected.

Abbreviations: CPMG – Carr-Purcell-Meiboom-Gill; CPP – cell-penetrating peptide; DHPC – 1,2-dihexanoyl-*sn*-glycero-3-phosphocholine; DHPC-d_{22} – deuterated 1,2-dihexanoyl-*sn*-glycero-3-phosphocholine; DMPC – 1,2-dimyristoyl-*sn*-glycero-3-phosphocholine; DMPC-d_{54} – deuterated 1,2-dimyristoyl-*sn*-glycero-3-phosphocholine; DMPG-d_{54} – deuterated 1,2-dimyrisotoyl-sn-glycero-3-[phospho-*rac*-(1-glycerol)]; HSQC – heteronuclear single quantum coherence; NMR – nuclear magnetic resonance; NOE – nuclear Overhauser enhancement; PNAs – peptide nucleic acids; siRNA – small interfering RNA

Introduction

Transportan is a 27 residues long peptide with the sequence: GWTLNSAGYLLGKINLKALAALAKKIL. It is a chimeric peptide constructed from 12 amino acid residues derived from the N-terminal part of the neuropeptide galanin linked with a lysine residue to the 14 amino acids of the wasp venom mastoparan (Pooga et al., 1998).

Transportan belongs to a group of peptides, called cell-penetrating peptides (CPPs), studied because of their ability to transport large covalently attached hydrophilic cargoes across the cell membrane. By investigating the details in the interaction between these peptides and the membrane, we can increase our understanding of the translocation mechanism. The aim of using CPPs is to enhance the efficiency, by increasing the uptake, of gene regulating drugs, such as peptide nucleic acids (PNAs) and small interfering RNA (siRNA) (Derossi et al.,

*To whom correspondence should be addressed.
E-mail: lena.maler@dbb.su.se

1998; Järver and Langel, 2004; Magzoub and Gräslund, 2004; Deshayes et al., 2005).

Gene-regulating drugs have their biological function in the nucleus, but are effectively hindered to reach the target by the membrane barrier. Hence, CPPs can play an important role in increasing the uptake of these hydrophilic molecules. The mechanism by which the peptide–cargo complex translocates across the membrane barrier is, however, still not completely understood. Endocytosis has been shown to be important in many cases (Lundberg and Johansson, 2002; Drin et al., 2003; Richard et al., 2003), but other mechanisms, such as direct electrostatic or membrane potential mediated penetration have also been proposed (Sakai and Matile, 2003; Terrone et al., 2003). It is known that most of the material brought in by endocytosis is transported directly to lysosomes for degradation, which is a problem since most of the cargo could be digested before it has reached the target. Transportan and related peptides are also known to be highly toxic, which could partly be explained by the lytic activity they have on membranes (Jones et al., 2005).

We have previously reported the structure of transportan when bound to phospholipid bicelles and it was found to be α-helical in the C-terminal mastoparan part of the peptide while the N-terminus is less structured but with significant helical character also in this part of the peptide (Bárány-Wallje et al., 2004). In the present study we characterize the interaction between the transportan peptide and model membranes, bicelles, by ^{15}N relaxation methods. Nuclear spin relaxation is sensitive to motions on the ps–ns time-scale, which are important for understanding the interaction between peptides and the membrane.

Bicelles are disk-shaped aggregates formed by mixing, e.g., long- and short-chained phospholipids. The relative composition of the mixture, which controls the size of the bicelle, is referred to as the q-ratio (ratio of the amount of phospholipid to detergent). Small isotropic bicelles (with $q < 0.5$) are suitable for high-resolution NMR studies of membrane interacting peptides (Vold et al., 1997). In this investigation, 1,2-dimyristoyl-*sn*-glycero-3-phosphocholine (DMPC) is used as the long-chained lipid while 1,2-dihexanoyl-*sn*-glycero-3-phosphocholine (DHPC) is used as the short-chained lipid. These zwitterionic phospholipids form stable bicelles over a relatively wide range of temperatures, concentrations and pH. Partly charged bicelles are obtained by replacing a fraction of the DMPC with negatively charged lipids, such as DMPG or DMPS (Vold and Prosser, 1996; Struppe et al., 2000; Glover et al., 2001).

In this study we show that the dynamics of the CPP transportan depends on the surface charge of the bicelle. By replacing a fraction (10%) of the DMPC with DMPG the overall dynamics of transportan is effectively slowed down, and the local dynamics is more restricted. To investigate the effect of the peptide on lipid dynamics we measured carbon-13 relaxation of DMPC and DHPC acyl chains in zwitterionic bicelles. Transportan is seen to influence both DMPC and DHPC dynamics.

Methods

Sample preparation

Transportan containing ^{15}N-labeled Leu residues (residues 4, 10, 11, 16, 19, 22 and 27) was obtained from Neosystem Labs and was used as received. The peptide was amidated at the C-terminus. Deuterated 1,2-dimyristoyl-*sn*-glycero-3-phosphocholine (DMPC-d_{54}), deuterated 1,2-dihexanoyl-*sn*-glycero-3-phosphocholine (DHPC-d_{22}) and deuterated 1,2-dimyrisotoyl-*sn*-glycero-3-[phospho-*rac*-(1-glycerol)] (DMPG-d_{54}) as well as undeuterated lipids were purchased from Avanti Polar Lipids.

Samples containing ^{15}N-labeled transportan were produced by first mixing peptide and DMPC powder in phosphate buffer (final concentration 50 mM, pH 5.5). A 1 M solution of DHPC-d_{22} was added to produce a sample with 1 mM peptide concentration, 300 mM total lipid concentration and q = [DMPC]/[DHPC] = 0.33. The sample was vortexed and transferred to an NMR tube. In order to produce negatively charged bicelles, 10% of the DMPC-d_{54} was exchanged for DMPG-d_{54}. About 10% D_2O (purchased from Aldrich) was added for field/frequency lock stabilization. Samples for measuring lipid dynamics and translational diffusion were prepared with unlabeled peptide and dissolved in 100% D_2O. These samples contained undeuterated DMPC and DHPC, 50 mM KCl, and the q-values was 0.25. We have previously used KCl instead of phosphate buffer and we have never observed any difference in peptide–bicelle interactions in bicelles with zwitterionic lipids (Andersson and Mäler, 2003).

NMR spectroscopy

Bruker Avance spectrometers, operating at magnetic field strengths of 9.39 and 11.74 T, and Varian Inova spectrometers, operating at magnetic fields of 14.09 T and 18.78 T were used. All spectrometers were equipped with triple-resonance probe-heads. The temperature was 37 °C during all experiments, as confirmed by calibration using ethylene glycol as a reference. Processing was done with the FELIX processing software (Accelrys, version 2000.1). A 3D ^{15}N-^{1}H NOESY-HSQC spectrum was recorded at 11.74 T using 2048 complex points in the direct ^{1}H dimension, 256 in the indirect ^{1}H dimension and 64 complex points in the indirect ^{15}N dimension using 8 scans and a mixing time of 100 ms.

Relaxation measurements were performed at 9.39, 14.09 and 18.78 T. R_1 and R_2 ^{15}N-relaxation rates were determined using sensitivity enhanced pulse sequences (Kay et al., 1992; Skelton et al., 1993). Typically, 2700×64 complex points were collected, using 32 scans. For determining R_1 relaxation rates, 10 different relaxation delays ranging between 0 and 2.56 s were used, and for measuring R_2 relaxation rates 10 delays between 0 and 0.25 s were used. Experiments with two relaxation delays (one long and one short) were measured twice in order to estimate the uncertainties of the relaxation rates. Data processing included zero-filling to 4096×2048 points and apodization with a 90° shifted sine-bell function prior to Fourier transformation. The relaxation rates were determined by a two-parameter exponential fit of the maximum peak intensities as well as the integrated peak volumes. The heteronuclear ^{15}N–^{1}H NOE factors were determined by recording spectra with zero seconds irradiation time (no NOE) and 8 s irradiation time (full NOE). Typically 2048×32 complex points using 128 scans were collected. The NOE factors were calculated by taking the ratio of the peak intensities obtained with the long irradiation period and the zero irradiation period. Uncertainties were estimated from duplicate experiments.

The chemical exchange on a millisecond timescale (Palmer III et al., 2001) was investigated using a Carr-Purcell-Meiboom-Gill (CPMG) sequence (Carr and Purcell, 1954; Meiboom and Gill, 1958) with enhanced sensitivity to chemical exchange (Wang et al., 2001). The variable delay, τ_{CPMG}, between pulses in the CPMG pulse sequence was set to 0.26 and 1.2 ms, respectively and R_2 was measured as described above for both cases.

The dynamics of both DMPC and DHPC within $q = 0.25$ bicelles was investigated by direct ^{13}C-detected steady-state NOE and R_1 relaxation measurements on natural abundance ^{13}C in the lipid acyl chains as described previously (Andersson and Mäler, 2005). NOE factors were recorded at 9.39 T, and R_1 values were recorded at 9.39 and 14.09 T in the absence of and in the presence of 10 mM transportan. The ^{13}C peaks for the fatty acyl chain carbons in DHPC were assigned as follows: carbon 2, 34.33/34.22 ppm; carbon 3, 24.79/24.69 ppm; carbon 4, 31.51/31.36 ppm; and carbon 5, 22.52/22.50 ppm. No attempt was made to individually assign the resonances belonging to the two different acyl chains.

The translational diffusion of transportan as well as diffusion of the lipids in the bicelles were measured at a magnetic field strength of 14.09 T using a pulsed field gradient spin echo pulse sequence (Stejskal and Tanner, 1965; Callaghan et al., 1998), as previously described (Andersson et al., 2004). The diffusion experiment was performed using 30 linearly incremented steps with increasing gradient power, up to maximum ~60 G/cm. A total of 16 transients were recorded for each step and a T_1-delay of 0.2 s was used. The gradient profile of the used probe-head was taken into account as described by Damberg et al. (2001). Translational diffusion coefficients were obtained by fitting peak integrals to the modified Stejskal–Tanner equation.

Hydrogen to deuterium exchange was measured using samples containing 1 mM transportan in bicelles made with either DMPC or DMPC/DMPG (10% DMPG). The samples were prepared as described above and freeze-dried to give a solid powder in the bottom of the NMR tube. The samples were dissolved in 600 μl of D_2O and then put directly into the NMR spectrometer. 2D ^{15}N–^{1}H HSQC spectra with 2048×64 complex points using 4 or 8 scans were recorded with 5 or 10 min intervals for as long as signals remained visible.

The relaxation data were analyzed with the model-free approach as stated by Lipari and Szabo (1982a, b). During the fitting procedure, the scheme by Mandel et al. (1995) was used. Thus,

starting from a simple model with only a global correlation time for each site, τ_i (assuming an isotropic overall rotation), and an order parameter, S^2, additional parameters were added until a good fit was obtained. The software Modelfree (Palmer III et al., 1991; Mandel et al., 1995) was used to model the spectral density function from the relaxation rates and their corresponding uncertainties. It is likely that an aggregate such as the bicelle–peptide complex will not undergo isotropic reorientation and therefore we fitted the overall dynamics individually for each ^{15}N–^{1}H bond vector. We did not find it necessary to use a term for chemical exchange in the evaluation of the R_2 data. Hence, the final parameters describing the motion at each of the seven sites investigated were a global correlation time (τ_i), a local correlation time (τ_e) and a squared generalized order parameter (S^2).

CD spectroscopy

CD spectra were recorded for 1 mM transportan in neutral bicelles and 10% negatively charged bicelles with q values of 0.33, as well as in 50 mM phosphate buffer (pH 5.6). Spectra were collected on a Jasco J-720 CD spectropolarimeter using a 0.05 mm quartz cuvette. Wavelengths ranging from 190 to 250 nm were scanned using a 0.2 nm step resolution and 100 nm/min speed. The temperature was controlled by a PTC-343 controller, and set to 37 °C. Spectra were collected and averaged over 16 scans. After subtraction of the solvent spectra the α-helical content was estimated from the mean residue molar ellipticity at 222 nm, assuming a two-state equilibrium between α-helix and random coil conformation, $\Theta_{\alpha-\mathrm{helix}} = -35,700$ deg cm^2/dmol, and $\Theta_{RC} = 3900$ deg cm^2/ dmol (Greenfield and Fasman, 1969).

Fluorescence spectroscopy

The tryptophan fluorescence was measured on a Perkin Elmer LS 50B Luminescence spectrometer. All measurements where made at room temperature in a quarts cuvette with a light path length of 0.5 mm (Dye-Laser Cells). The excitation wavelength was 280 nm and the emission was scanned from 300 to 500 nm. Ten scans were collected with a scan speed of 600 nm/min. The excitation bandwidth as well as the emission bandwidth was 10 nm. Samples containing 1 mM transportan in neutral as well as in 10% negatively charged $q = 0.33$ bicelles were titrated with acrylamide. Acrylamide was added from a 1 M stock solution, resulting in concentrations between 20 and 500 mM. Quenching constants (K_{SV}) were determined by a linear regression with the Stern–Volmer equation for a dynamic process (Lakowicz, 1999):

$$\frac{F}{F_0} = 1 + K_{SV}[Q] \quad (1)$$

where F and F_0 are the fluorescence intensities in the presence and absence of acrylamide, and $[Q]$ is the concentration of acrylamide.

Results

Transportan–bicelle interaction

CD was used to compare the structure of transportan in zwitterionic and partly negatively charged bicelles, and the CD spectra for transportan in the two bicelles and in phosphate buffer are depicted in Figure 1. The α-helical content was 38% in neutral bicelles, 42% in charged bicelles and 25% in phosphate buffer respectively, as estimated from the mean residue molar ellipicities at 222 nm which were; −11,119 deg cm^2/dmol (in neutral bicelles), −12,539 deg cm^2/dmol (in charged bicelles) and −5858 deg cm^2/dmol (in phosphate buffer), respectively. The structure in charged bicelles thus seems to be similar to the one found in neutral bicelles (Bárány-Wallje et al., 2004).

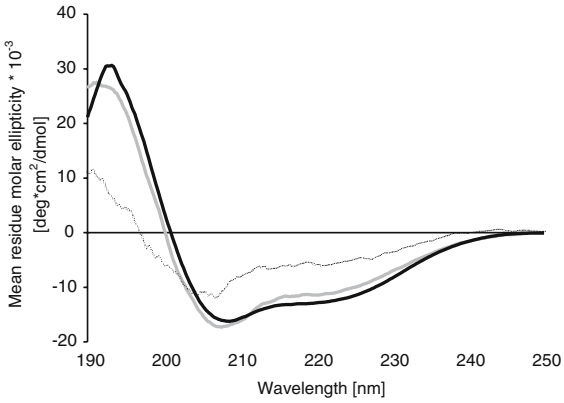

Figure 1. CD-spectra of transportan in neutral bicelles (solid grey line), charged bicelles (black line) and 50 mM phosphate buffer, pH 5.6 (dashed grey line) recorded at 37 °C.

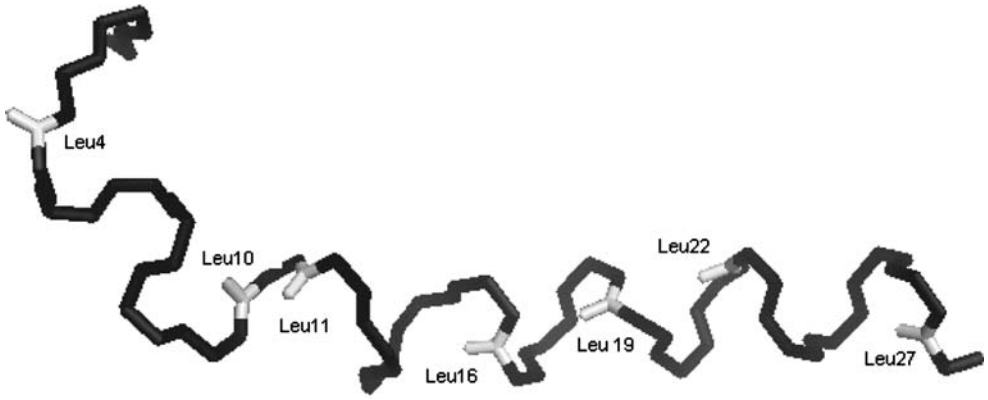

Figure 2. The structure of transportan with the seven ^{15}N–^{1}H vectors of the leucine residues labeled in grey. The structure was obtained from the protein data bank (http://www.rcsb.org/pdb/) under the accession code 1SMZ.

Instrinsic Trp fluorescence of Trp2 in transportan was measured in both bicelle solvents as a function of increasing concentration of the external quencher acrylamide. A blue-shift in emission wavelength from 355 nm in buffer to 345 nm was observed in both samples, indicating interaction between transportan and the bicelles. The Stern–Volmer quenching constant for transportan in buffer or water solution is 31 M^{-1} (Magzoub et al., 2001), and any interaction with the bicelles would result in a reduction of the quenching constant. Here, we see a large reduction in K_{SV} for transportan in either bicelle solution, to 5.7 M^{-1} in neutral bicelles and to 5.5 M^{-1} in charged bicelles. The values are very similar in the two solvents, indicating a similar binding affinity, independent of charge, to the two bicelles. It has previously been demonstrated that transportan binds in a similar way to vesicles with different charges (Magzoub et al., 2001).

The seven Leu residues in transportan (4, 10, 11, 16, 19, 22 and 27) were specifically labeled with ^{15}N (Figure 2) and the HSQC spectrum consists of seven well-resolved cross-peaks (Figure 3). Assignments for the protons were available from previous investigations (Bárány-Wallje et al., 2004) and a three-dimensional ^{15}N–^{1}H NOESY-HSQC spectrum was collected in order to assign the backbone amide nitrogen resonance frequencies. The chemical shifts for transportan in neutral and negatively charged bicelles were found to be almost identical, which supports the conclusion that the peptide structure is similar in the two types of bicelles. The peaks were significantly broader when the peptide was bound to the charged bicelles, indicating differences in dynamics.

Amide hydrogen to deuterium exchange was studied by examining the ^{15}N–^{1}H HSQC spectrum of the ^{15}N–Leu labeled transportan dissolved in either zwitterionic bicelles or in bicelles in which 10% of the DMPC was replaced with DMPG. The purpose of these investigations was to qualitatively determine protection factors for the amide protons. Spectra were recorded with time intervals of 5 min for transportan in zwitterionic bicelles and 10 min for transportan in partly negatively charged bicelles. The reason for recording longer

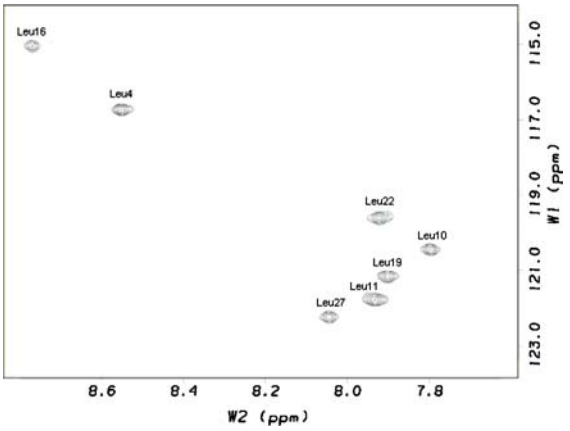

Figure 3. An assigned ^{15}N–^{1}H HSQC spectrum of transportan in neutral bicelles (q = 0.33) recorded at 37 °C.

Table 1. Correlation times and squared generalized order parameters for the seven residues labeled with ^{15}N as estimated from the measured relaxation rates through the model-free approach.

Residue	Neutral bicelles			Charged bicelles		
	τ_i (ns)	S^2	τ_e (ns)	τ_i (ns)	S^2	τ_e (ns)
4	16.1 ± 0.9	0.42 ± 0.02	1.6 ± 0.08	17.8 ± 0.7	0.62 ± 0.02	1.5 ± 0.1
10	14.8 ± 0.8	0.70 ± 0.02	1.5 ± 0.2	18.3 ± 0.8	0.80 ± 0.02	1.4 ± 0.2
11	12.6 ± 0.4	0.77 ± 0.02	1.1 ± 0.1	16.4 ± 0.6	0.80 ± 0.02	1.3 ± 0.2
16	16.2 ± 1	0.71 ± 0.03	1.6 ± 0.2	16.8 ± 1	0.90 ± 0.06	–
19	13.5 ± 0.5	0.83 ± 0.02	1.5 ± 0.3	17.5 ± 0.7	0.87 ± 0.02	1.7 ± 0.5
22	13.9 ± 0.5	0.80 ± 0.02	1.3 ± 0.2	18.3 ± 0.8	0.86 ± 0.03	2.9 ± 2
27	14.2 ± 0.7	0.77 ± 0.02	1.4 ± 0.2	16.3 ± 0.8	0.91 ± 0.03	1.3 ± 0.4

HSQC spectra in charged bicelles was that the peaks were heavily broadened in this solvent, and thus longer experiment times were required to obtain reasonable signal to noise.

After 5 min, all seven peaks were still visible in the spectrum for transportan in zwitterionic bicelles. The peaks gradually disappear as the protons exchange for deuterons, starting with the most terminal residues Leu4 and Leu27. After 15 min only peaks corresponding to Leu11, Leu19 and Leu22 remained. After 30 min all the peaks had disappeared completely, which is significantly faster than what has been observed for other helical bicelle-bound peptides that reside orthogonal to the bicelle surface (Biverståhl et al., 2004; Papadopoulos et al., 2006).

For transportan in partly negatively charged DMPC/DMPG bicelles, the results were very similar to those in zwitterionic DMPC bicelles. After 10 min, all signals remained, after 20 min only signals corresponding to Leu11, Leu19 and Leu22 remained, and all signals had completely disappeared after 30 min, indicating very similar exchange behaviour for the amide protons in transportan in the two bicelle solvents.

Dynamics of transportan

The R_1, R_2 and NOE relaxation parameters for the peptide were determined at three different magnetic field strengths in neutral bicelles as well as in charged bicelles (supplementary material). The relaxation data was then used to model the spectral density function as described by Lipari and Szabo (1982a, b) assuming an isotropic overall rotation of each of the sites in the peptide. Starting from a simple model with only two parameters (a global correlation time and an order parameter) we added additional fitting-parameters until a good fit was obtained (Mandel et al., 1995). The final fit was made with a global correlation time (τ_i) for each site (i), a local correlation time (τ_e) and a squared generalized order parameter (S^2) to describe the motion of transportan. The results of this fit are collected in Table 1. As an example of the fit, the calculated relaxation rates for Leu19 together with the experimentally determined values are shown in Figure 4.

We did not find it necessary to use an R_{ex} term in the fit described above, but to ascertain that the peptide does not undergo fast intermediate chemical exchange, presumably between a free and bound form, we determined the effect of exchange on R_2 by using the method developed by Wang et al. (2001). The measured R_2 rates were found to be the same when using different delays between the pulses in the CPMG pulse train, τ_{CPMG} (0.26 and 1.2 ms). Thus, no chemical exchange was detected in the investigated time window. Furthermore, we cannot detect any signals in the spectrum originating from a population of free peptide, which would be the case for slow exchange between a free and bound form. This indicates, in agreement with the fluorescence results that the extent of the interaction between transportan and lipids is independent of charge, and that no significant population of the free form can be seen in either bicelle solvent.

Turning to the results of the model-free fit, several conclusions can be made. The order parameter for residue 4 is lower in both bicelle solvents than the corresponding values found for

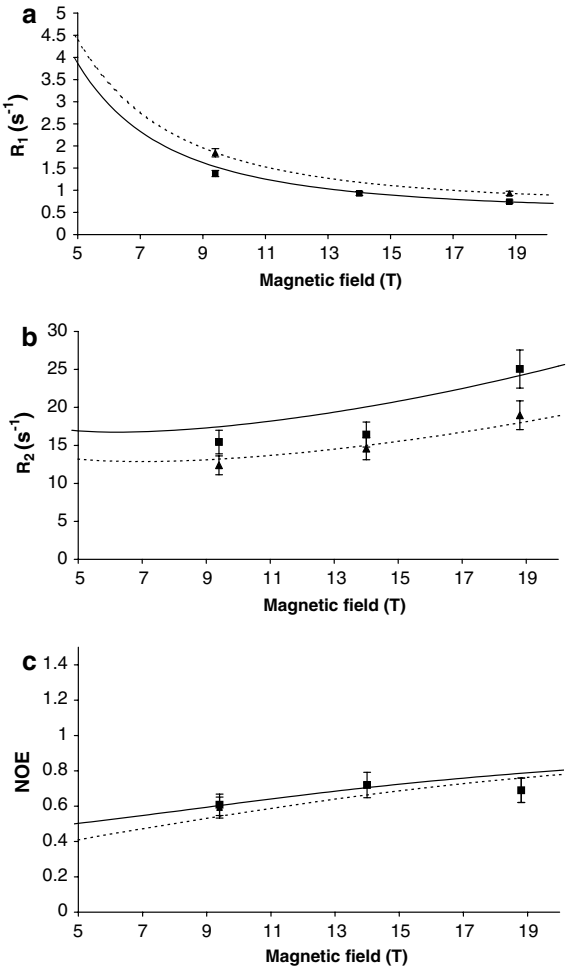

Figure 4. Relaxation data for Leu19 in transportan. Squares denote measured values in charged bicelles and triangles denote measured values in neutral bicelles. The theoretically expected field-dependences of R_1, R_2 and NOE were calculated using the correlation times and squared generalized order parameters of Leu19 (shown in Table 1) and are depicted as solid lines (charged bicelles) and dashed lines (neutral bicelles). (a) calculated and measured R_1 values (b) calculated and measured R_2 values (c) calculated and measured NOE values.

the other residues, indicating that the N-terminus is more flexible than the rest of the peptide. This is expected since the structure of the peptide suggests a more flexible N-terminus. In fact, all of the residues belonging to the N-terminal galanin part of the peptide show lower order parameters than the mastoparan part. Both the order parameters and global correlation times are for all residues significantly higher for transportan in charged bicelles as compared to in zwitterionic bicelles. An average increase of 3 ± 1 ns in global correlation time and 0.11 ± 0.07 in order parameter squared is observed. This shows that the effective tumbling rate for the peptide becomes slower, and that transportan is a more rigid object when bound to charged bicelles as compared to neutral bicelles.

Lipid dynamics

By adding 10 mM transportan to $q = 0.25$ bicelles it is clearly seen that the peptide influences the ^{13}C R_1 and NOE relaxation of DMPC and DHPC both at 9.39 T and 14.09 T. Figure 5 shows the effect of transportan on lipid dynamics for DMPC (positions 2, 3, 12 and 13 in the acyl chains) as well as DHPC (positions 2, 3, 4 and 5 in the acyl chains) at 9.39 T. Relaxation data for carbons in the two acyl chains are shown, but no attempt was made to individually assign them. In general there are large differences between the data observed for the two chains, indicating very different dynamics.

The R_1 values for all measured sites (carbons 2, 3, 12 and 13 in DMPC and 2, 3, 4, 5 in DHPC) in DMPC and DHPC are affected by the addition of transportan. An increase in the R_1 values is observed throughout the acyl chain of both DMPC and DHPC. R_1 data were also collected at 14.09 T, and the values were generally lower than at 9.39 T as expected from the field-dependence of the relaxation rates seen previously (Andersson and Mäler, 2005), but overall show a similar trend in the peptide-induced effect on relaxation.

The heteronuclear NOE is a sensitive measure of changes in local dynamics. Transportan has a somewhat confusing effect on the NOE factors measured for the acyl chains in DMPC. The peptide is seen to on average lower the NOE factors, indicating that the lipids become more rigid. More striking is the observation that transportan seems to make the dynamics in the two acyl chains more different, as the difference in NOE factor is increased by adding peptide. Although lower order parameters are observed also for DHPC in the presence of transportan, the same effect leading to differences in NOE factors for the acyl chains is not observed for DHPC.

Taken together these data show that the presence of transportan clearly influences the dynamics of both DMPC and DHPC. The uniform perturbation in R_1 values indicates that parameters that influence the dynamics of the entire lipid molecule are affected. Such parameters include the

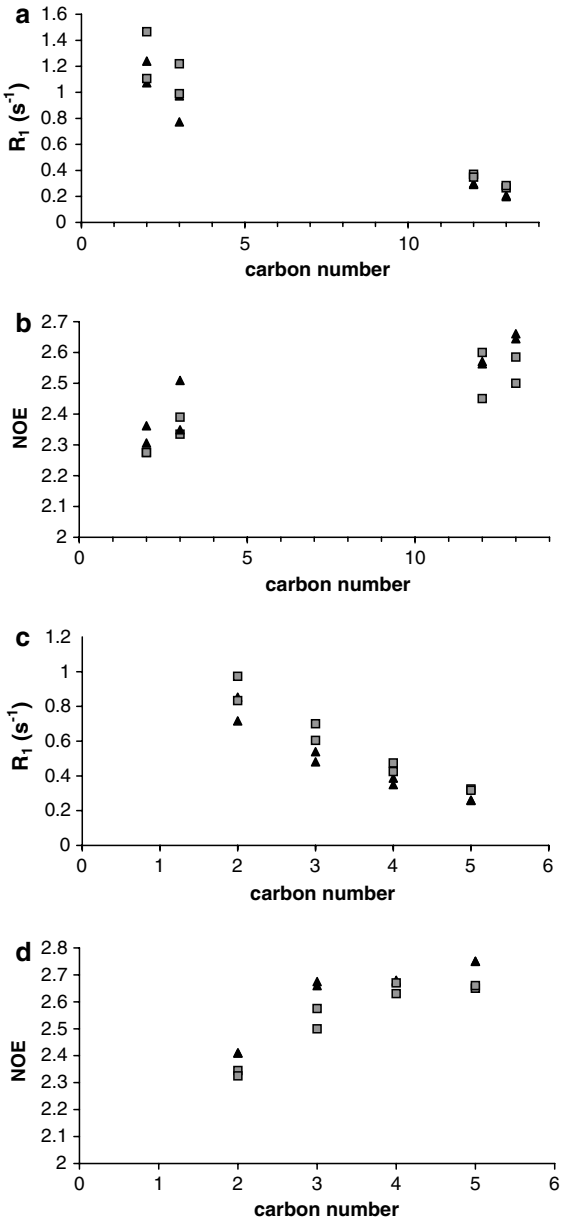

Figure 5. ^{13}C relaxation data for DMPC and DHPC in $q = 0.25$ DMPC/DHPC bicelles measured at 9.4 T. Black triangles indicate data for bicelles without transportan and grey squares data for bicelles with 10 mM transportan. Both lipids have two hydrocarbon chains that are different enough to give rise to separate peaks. (a) R_1 for the acyl chain carbons in DMPC; (b) NOE for the acyl chain carbons in DMPC; (c) R_1 for the acyl chain carbons in DHPC; (d) NOE for the acyl chain carbons in DHPC.

rotational correlation time for the lipids, the order parameter for the entire lipid and the lateral diffusion of the lipid on the surface of the aggregate. Furthermore, the peptide is seen to affect the local dynamics of the two acyl chains in DMPC in different ways, which can be explained if transportan interacts selectively with DMPC.

Diffusion

By comparing relative diffusion of different components in the sample it is possible to monitor the degree of binding to the bicelle, as has been described previously (Andersson and Mäler, 2003). About 10 mM transportan was added to DMPC $q = 0.25$ bicelles. The diffusion of the bicelles, as monitored by DMPC diffusion, without transportan was $7.3 \cdot 10^{-11}$ m^2/s (Andersson and Mäler, 2005), whereas the diffusion of the bicelles in the presence of peptide was $4.5 \cdot 10^{-11}$ m^2/s. The diffusion of transportan in the bicelles was $4.0 \cdot 10^{-11}$ m^2/s. This means that transportan alters the bicelle size, and that DMPC diffuses slightly faster than transportan, indicating that all of the peptide is bicelle bound, while there are bicelles without transportan.

Assuming, according to the reasoning above, and the previous results, that all transportan molecules bind to the bicelles, this allows us to calculate the fraction of bicelles (x) where transportan is present according to the relationship:

$$D_{\text{bicelle+transportan}} = x \cdot D_{\text{transportan}} + (1 - x) \cdot D_{\text{bicelle}} \quad (2)$$

which in the present case gives us $x = 0.85$. This means that transportan influences the lipid dynamics in 85% of the bicelles.

Discussion

The present study focuses on the surface charge-dependence of transportan dynamics in bicelles. In order to correctly assess the influence of different charge density on dynamic parameters it is important to first establish what the differences in structure and extent of membrane interaction of transportan in the two bicelles are. The structure of transportan, as judged from CD spectra, is very similar in neutral bicelles and charged bicelles (Figure 1). The similarity of the structure in the two solvents is confirmed by the chemical shifts of H^{α}, H^{N} and ^{15}N, which are almost identical in the two bicelles.

In order to examine the relaxation data, the amount of peptide that binds to the two bicelles must be established. Very similar amide proton exchange rates for transportan in the two bicelles, which are faster than 30 min for all amide protons, indicate that transportan is located in the headgroup region at the surface of both bicelles, and is bound to a similar extent to both bicelles. This is in contrast to peptides positioned in a transmembrane configuration, which do not show any significant amide proton exchange in the helical part buried within the bicelle interior (Biverståhl et al., 2004; Papadopoulos et al., 2006). The fluorescence quenching measurements confirm the amide proton exchange results, showing that transportan binds to a large extent to both bicelles, showing very small differences in quenching constants for Trp2 in the two bicelles. The translational diffusion measurements indicate that all the peptide is bound to the zwitterionic bicelles, and that some of the bicelles do not contain peptide.

Previous investigations of the interaction between transportan and vesicles with different charge density have shown that transportan binds to membrane surfaces in a charge-independent way (Magzoub et al., 2001). Hence, we conclude that the extent of the interaction between the peptide and the two bicelle solvents can safely be assumed to be similar, and that most of the peptide is bound. We see no evidence in the NMR data of a population of free peptide exchanging with the bound state on the fast exchange time-scale.

Turning to the dynamics, we see that negatively charged bicelles impose a restriction of peptide motion as compared to the zwitterionic bicelles. The overall correlation time (τ_i) for each site (i), related to an effective correlation time for the entire peptide motion in the bicelle, is significantly slower in the presence of negatively charged bicelles (Table 1). Thus, the apparent tumbling of the peptide becomes slower in the charged bicelle, and is accompanied by more restricted local dynamics.

There may be several reasons for the observed difference in overall dynamics. Transportan may in fact alter the composition of the two bicelles in different ways depending on whether it is bound to neutral or negatively charged bicelles, leading to differences in bicelle size, and thus to differences in bicelle tumbling. A second reason for observing slower tumbling rates is that the overall motion of the peptide is not the same in the two bicelle solvents.

In both neutral and charged bicelles there are also subtle differences in global correlation times for the individual sites in transportan, indicating motional anisotropy. From examining the structure, we can see that the Leu residues in the C-terminal mastoparan part of the peptide are more or less positioned in the same orientation. This part of the peptide structure is fairly well-defined and shows the characteristic NOE cross-peak patterns for an α-helical structure. The first three Leu residues in the N-terminus, however, have a different orientation. The N-terminal part of the structure is not as well-defined, but a number of NOE constraints indicating helical structure were also found for this part of the peptide, and ϕ and ψ torsion angles in the helical range were observed for residues Asn5 through Gly8 (Bárány-Wallje et al., 2004).

Keeping in mind that the structure is poorly defined in the N-terminus, and the limited variation of bond vector orientations available in the peptide, we nevertheless made an attempt to analyze the anisotropy in the peptide motion from the individual global correlation times associated with the ^{15}N–^{1}H bond vectors. The analysis was made using the program Quadric diffusion (Lee et al., 1997).

Assuming an axially symmetric diffusion tensor, we see that transportan in the zwitterionic bicelles behaves as if it had a prolate shape (Figure 6), indicating that the peptide has a large degree of rotational freedom around the molecular long axis in the bicelle. The diffusion tensor for the peptide in negatively charged bicelles, in contrast, has an oblate form. This indicates that the peptide is more rigid when attached to the negatively charged bicelle, or at least more restricted in the motion around the molecular long axis than in the case of neutral bicelles. Hence, the analysis reveals significant differences in the interaction between the peptide and the two different bicelles.

The difference in dynamic behavior (and hence the relaxation parameters) of transportan when bound to charged bicelles compared to neutral bicelles explains why we had difficulties in recording well-resolved proton NMR spectra in charged bicelles while the spectra in neutral bicelles were of good quality. The relaxation parameters depend on a combination of factors

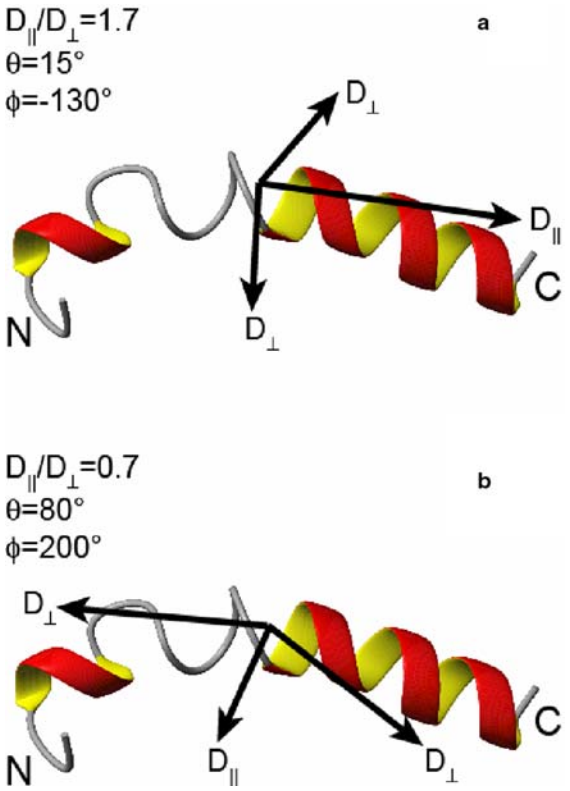

Figure 6. The principal axes of the axially symmetric diffusion tensor for transportan in neutral bicelles (a) and in 20% negatively charged bicelles (b). The relative magnitudes of the components $D_{||}$ and $D_{\perp}$ are shown relative to the moment of inertia tensor calculated for transportan. The calculated values for $D_{||}/D_{\perp}$, and are shown. The figure was produced using Molmol (version 2.6) and the structure was taken from the PDB (accession code 1SMZ). The helical parts of the structure are indicated with ribbons.

such as increased rigidity of the lipids, mobility of the peptide within the bilayer, and on the specific dynamical properties of the peptide (Andersson and Mäler, 2005).

Adding transportan to neutral bicelles affects the dynamics of both bicelle constituents (DHPC and DMPC). The R_1 values both for DMPC and DHPC increase in the presence of peptide while the NOE factors for DMPC decrease in presence of peptide for all residues studied. It has previously been shown that these relaxation parameters do not reflect differences in the size of the bicelle aggregates (Andersson and Mäler, 2005), as the reorientation of the bicelle is too slow to affect the R_1 and NOE parameters. The uniform perturbation instead indicates that parameters that influence the dynamics of the entire lipids are affected when transportan is added.

It is also interesting to note that transportan has the effect of increasing the difference in local dynamics for the two acyl chains in the DMPC molecule. This indicates that transportan affects the dynamics of both DMPC and DHPC, but in different ways. The overall reorientation of both molecules seem to be affected while the local dynamics of the DMPC acyl chain is more affected by transportan. One should keep in mind that there is a possibility is that the overall morphology of the bicelle might be distorted by the peptide.

In conclusion we find that the dynamics on the ps–ns time-scale of the cell-penetrating peptide transportan depends on the charge of the bicelle. Both local motion and overall rotation is affected, indicating a more rigid bicelle–peptide complex in the case of negatively charged bicelles. These changes are not reflected in the structure of the peptide. It is also found that the presence of the peptide alters the relaxation parameters of the lipids (DHPC and DMPC, respectively) in the bicelle, which shows that transportan affects overall lipid motion as well as local motion within the DMPC acyl chains.

Electronic supplementary material is available in electronic format at http://dx.doi.org/10.1007/s10858-006-9008-y.

Acknowledgements

We wish to thank Joshua Hicks for helpful insights and careful reading of the manuscript. This work is supported by grants from the Swedish Research Council and the Carl Trygger Foundation.

References

Andersson, A., Almqvist, J., Hagn, F. and Mäler, L. (2004) *Biochim. Biophys. Acta*. **1661**, 18–25.
Andersson, A. and Mäler, L. (2003) *FEBS Lett*. **545**, 139–143.
Andersson, A. and Mäler, L. (2005) *Langmuir* **21**, 7702–7709.
Bárány-Wallje, E., Andersson, A., Gräslund, A. and Mäler, L. (2004) *FEBS Lett*. **567**, 265–269.
Biverståhl, H., Andersson, A., Gräslund, A. and Mäler, L. (2004) *Biochemistry* **43**, 14940–14947.
Callaghan, P., Komlosh, M. and Nydén, M. (1998) *J. Magn. Reson*. **133**, 177–182.

Carr, H.Y. and Purcell, E.M. (1954) *Phys. Rev.* **94**, 630–638.
Damberg, P., Jarvet, J. and Gräslund, A. (2001) *J. Magn. Reson.* **148**, 343–348.
Derossi, D., Chassaing, G. and Prochiantz, A. (1998) *Trends Cell Biol.* **8**, 84–87.
Deshayes, S., Morris, M.C., Divita, G. and Heitz, F. (2005) *Cell. Mol. Life Sci.* **62**, 1839–1849.
Drin, G., Cottin, S., Blanc, E., Rees, A.R. and Temsamani, J. (2003) *J. Biol. Chem.* **278**, 31192–31201.
Glover, K.J., Whiles, J.A., Wu, G., Yu, N.-J., Deems, R., Struppe, J.O., Stark, R.E., Komives, E.A. and Vold, R.R. (2001) *Biophys. J.* **81**, 2163–2171.
Greenfield, N. and Fasman, G.D. (1969) *Biochemistry* **8**, 4108–4116.
Järver, P and Langel, Ü. (2004) *Drug Discov. Today.* **9**, 395–402.
Jones, S.W., Christison, R., Bundell, K., Voyce, C.J., Brockbank, S.M.V., Newham, P. and Lindsay, M.A. (2005) *Br. J. Pharmacol.* **145**, 1093–1102.
Kay, L.E., Keifer, P. and Saarinen, T. (1992) *J. Am. Chem. Soc.* **114**, 10663–10665.
Lakowicz, J.R. (1999) *Principles of Fluorescence Spectroscopy* (2nd ed.). Kluwer Academic New York.
Lee, L.K., Rance, M., Chazin, W.J. and Palmer, A.G. III (1997) *J. Biomol. NMR* **9**, 287–298.
Lipari, G. and Szabo, A. (1982a) *J. Am. Chem. Soc.* **104**, 4546–4559.
Lipari, G. and Szabo, A. (1982b) *J. Am. Chem. Soc.* **104**, 4559–4570.
Lundberg, M. and Johansson, M. (2002) *Biochem. Biophys. Res. Commun.* **291**, 367–371.
Magzoub, M. and Gräslund, A. (2004) *Q. Rev. Biophys.* **37**, 147–195.
Magzoub, M., Kilk, K., Eriksson, L.E.G., Langel, Ü. and Gräslund, A. (2001) *Biochim. Biophys. Acta* **1516**, 77–89.
Mandel, A.M., Akke, M. and Palmer, A.G. III (1995) *J. Mol. Biol.* **246**, 144–163.
Meiboom, S. and Gill, D. (1958) *Rev. Sci. Instrum.* **29**, 688–691.
Palmer, A.G. III, Kroenke, C.D. and Loria, P.J. (2001) *Meth. Enzymol.* **339**, 204–238.
Palmer, A.G. III, Rance, M. and Wright, P. (1991) *J. Am. Chem. Soc.* **113**, 4371–4380.
Papadopoulos, E., Oglecka, K., Mäler, L., Jarvet, J., Wright, P.E., Dyson, J. and Gräslund, A. (2006) *Biochemistry* **45**, 159–166.
Pooga, M., Hällbrink, M., Zorko, M. and Langel, Ü. (1998) *FASEB J.* **12**, 67–77.
Richard, J.P., Melikov, K., Vives, E., Ramos, C., Verbeure, B., Gait, M.J., Chernomordik, L.V. and Lebleu, B. (2003) *J. Biol. Chem.* **278**, 585–590.
Sakai, N. and Matile, S. (2003) *J. Am. Chem. Soc.* **125**, 14348–14356.
Skelton, N.J., Palmer, A.G. III, Akke, M., Kördel, J., Rance, M. and Chazin, W.J. (1993) *J. Magn. Reson. B.* **102**, 253–264.
Stejskal, E.O. and Tanner, J.E. (1965) *J. Chem. Phys.* **42**, 288–292.
Struppe, J., Whiles, J.A. and Vold, R.R. (2000) *Biophys. J.* **78**, 281–289.
Terrone, D., Sang, S.L.W., Roudaia, L. and Silvius, J.R. (2003) *Biochemistry.* **42**, 13787–13799.
Vold, R.R. and Prosser, R.S. (1996) *J. Magn. Reson. B.* **113**, 267–271.
Vold, R.R., Prosser, S.R. and Deese, A.J. (1997) *J. Biomol. NMR* **9**, 329–335.
Wang, C., Grey, M.J. and Palmer, A.G. III (2001) *J. Biomol. NMR* **21**, 361–366.